TISSUE ENGINEERING: Part A
Volume 19, Numbers 11 and 12, 2013

DOI: 10.1089/ten.tea.2012.0323

Characterization of Adipose-Derived Mesenchymal Stem Cell Combinations for Vascularized Bone Engineering

Cristian D. Valenzuela, MD,[1] Alexander C. Allori, MD, MPH,[1] Derek D. Reformat, MD,[1]
Alexander M. Sailon, MD,[1] Robert J. Allen, Jr., MD,[1] Edward H. Davidson, MBBS,[1]
Mani Alikhani, DDS, PhD,[2] Timothy G. Bromage, PhD,[3]
John L. Ricci, PhD,[3] and Stephen M. Warren, MD[1]

Since bone repair and regeneration depend on vasculogenesis and osteogenesis, both of these processes are essential for successful vascularized bone engineering. Using adipose-derived stem cells (ASCs), we investigated temporal gene expression profiles, as well as bone nodule and endothelial tubule formation capacities, during osteogenic and vasculogenic ASC lineage commitment. Osteoprogenitor-enriched cell populations were found to express *RUNX2*, *MSX2*, *SP7* (osterix), *BGLAP* (osteocalcin), *SPARC* (osteonectin), and *SPP1* (osteopontin) in a temporally specific sequence. Irreversible commitment of ASCs to the osteogenic lineage occurred between days 6 and 9 of differentiation. Endothelioprogenitor-enriched cell populations expressed *CD34*, *PECAM1* (*CD31*), *ENG* (*CD105*), *FLT1* (Vascular endothelial growth factor [*VEGFR1*]), and *KDR* (*VEGFR2*). Capacity for microtubule formation was evident in as early as 3 days. Functional capacity was assessed in eight coculture combinations for both bone nodule and endothelial tubule formation, and the greatest expression of these end-differentiation phenotypes was observed in the combination of well-differentiated endothelial cells with less-differentiated osteoblastic cells. Taken together, our results demonstrate vascularized bone engineering utilizing ASCs is a promising enterprise, and that coculture strategies should focus on developing a more mature vascular network in combination with a less mature osteoblastic stromal cell.

Introduction

Blood supply is essential for bone formation, repair, and regeneration. Studies of *de novo* bone formation have shown that new blood vessel formation precedes morphologic evidence of bone formation,[1] and the cytokine-release profile during the early stages of bony healing is largely angiogenic rather than osteogenic.[2] In murine models and in humans, marrow-derived endothelial progenitor cells (EPCs) and osteoprogenitor cells (OPCs) migrate to distant sites of injury or healing (e.g., fracture or distraction osteogenesis).[3–7] *In vivo* research has been limited by the fact that neovascularization is a complex process dependent on a conducive microenvironment consisting of optimal oxygenation, growth factors, and cell–cell interactions.[8–11] Additionally, studying bone formation in two-dimensional (2D) monoculture is hindered by the mineralized nature of the bone matrix, and recapitulating this process *in vitro* has proven difficult.[8]

Since engineered three-dimensional (3D) bone tissue constructs require adequate chemotransportation, development of an early vascular network within the tissue construct will be necessary. It is important to note, that the need for adequate chemotransportation is not only dependent on the composite tissue volume, but also on the changes in individual cellular requirements. For example, it has recently been shown that during mesenchymal stem cell (MSC) osteoinduction, there is a nearly threefold increase in oxygen consumption.[12] Osteodifferentiating MSCs consume more oxygen as they expand their mitochondrial-to-cytoplasm area to meet their needs as soon-to-be stromal cells (e.g., upregulation of secreted extracellular matrix proteins).[12]

This article was presented as an abstract at the American College Surgeons meeting in October 2009. Allori, A.C., Reformat, D.D., Davidson, E.H., Allen, R.J., Sailon, A.M., Valenzuela, C.D., Saadeh, P.B., Levine, J.P., Ricci, J.L., and Warren, S.M. "Functional analysis of simultaneous dual-differentiation vs multilineage cell coculture for vascularized bone engineering."
[1]Institute of Reconstructive Plastic Surgery Laboratories, New York University Langone Medical Center, New York, New York.
[2]Departments of Orthodontics and [3]Biomaterials and Biomimetics, New York University College of Dentistry, New York, New York.

Thus, as we decide upon the cellular coculture combinations for 3D bone constructs, it will be of critical importance to provide an early progenitor cell population capable of creating vascular networks for adequate chemotransportation.

Most strategies for bone engineering to date have focused on the principal stromal cell alone or on modulating osteoblastic function by incorporating osteogenic growth factors into scaffold constructs, leaving neovascularization to occur secondarily.[7,13–15] Recently, however, several groups have embedded vasculogenic factors (e.g., VEGF) into constructs in attempts to enhance vascular ingrowth *in situ*, and consequently improve osteogenesis.[16,17] Results are mixed, but there is some evidence this approach can result in inosculation between host circulation and the neovascularized scaffolds.[18] In contrast to relying on *in situ* neovascularization, some researchers have studied exogenous prevascularization of tissue-engineered constructs to improve the viability of the construct after implantation.[19,20]

Several laboratories have proposed coculture of osteogenic and vasculogenic cells, although the choice of cell combinations used has varied widely: for example, osteoblasts (OBs) with endothelial cells (ECs),[21] MSCs with ECs,[22,23] MSCs with EPCs,[24] and OPCs with ECs.[25] Similarly, the choice of tissue for cell sourcing is equally varied, including the recent use of adipose-derived stromal cells.[26–31] However, irrespective of the cell source, the coculture approach appears promising. For example, Kolbe *et al.* demonstrated that MSCs cocultured with ECs form robust vascular structures with upregulation of endothelial markers when cultured in vascular differentiation media, while significant mineralization with alkaline phosphatase upregulation occurs when cultured in osteogenic differentiation media (ODM).[32] However, many questions still exist regarding which media is optimal for coculture, which cell combination is most effective, which stem cell source is optimal, or whether neovascularization and osteogenesis should occur concurrently or consecutively.

We propose that the creation of an engineered bony tissue construct large and robust enough to solve clinical problems will depend on a prevascularized network to maintain viability. Therefore, attempts at bioengineered composite bone should include cocultured osteogenic and vasculogenic cell types. As an alternative to bone marrow-derived MSCs, Zuk *et al.* demonstrated that stem cells derived from lipoaspirate could be differentiated into adipogenic, vasculogenic, myogenic, chondrogenic, osteogenic, and even neuronal cell types in the presence of appropriate lineage-specific induction factors.[26–31] For practical application, the adipose-derived stem cell (ASC) is increasingly favored over bone marrow-derived MSC due to the relative ease of tissue harvest as well as the therapeutic side effect on the waistline. In the present study, we explore the plasticity and lineage commission of ASC-derived osteoprogenitor-enriched cell (OPEC) and endothelial progenitor-enriched cell (EPEC) populations. Enriched, in this context, refers to a heterogeneous cell population comprising of a spectrum of cells spanning along a differentiation lineage—from pluripotent mesenchymal cells to fully end-differentiated cells, including a significant population of osteoprogenitor and EPCs. We investigate eight coculture combinations to learn whether optimal cell combinations exist for vascularized bone engineering.

Materials and Methods

ASC isolation and expansion

Stromal stem cells were isolated and expanded from human lipoaspirate as previously described.[27,33] Cell culture media for all experiments are summarized in Table 1. A stem cell growth medium includes the Dulbecco's modified Eagle's medium (DMEM) and 50% fetal bovine serum (FBS). The stem cell expansion medium is similar to the above, but instead uses 10% FBS. ODM is comprised of the stem cell expansion medium with 0.01 nM dexamethasone and 20 nM ascorbate added, and aims to direct cell differentiation to the osteogenic route. The vasculogenic differentiation medium (VDM) includes components from the EGM-2 MV BulletKit in proprietary concentrations (Lonza, Basel, Switzerland), and aims to direct cell differentiation to the vasculogenic route. Briefly, human lipoaspirate was obtained from seven female donors (ages 18–55) (Institutional Review Board [IRB] approval #H12756-01b). Each patient received information about the scope and goals of this study. According to the IRB protocol, verbal informed consent was obtained before surgery. The specimens were collected as discarded tissue from patients undergoing elective lipoaspiration. After harvest, all samples were de-identified before processing. There was no collection of personal health information, demographic data, or other identifying data.

Each triplicate experiment utilized cells from one donor. Crude lipoaspirate was washed three times with the Hank's balanced saline solution (HBSS) (Invitrogen/Gibco,

Table 1. Cell Culture Media

Cell culture medium	*Composition*
Stem cell growth medium	DMEM (Fisher) 50% FBS (Invitrogen/Gibco) 1% antibiotic–antimycotic (Sigma-Aldrich)
Stem cell expansion medium	DMEM + 10% FBS
Osteogenic differentiation medium (ODM)	DMEM 10% FBS 0.01 mM dexamethasone 20 mM ascorbate
Mineralization medium (for Von Kossa assay)	DMEM 10% FBS 20 mM ascorbate 10 mM β-glycerophosphate (Sigma-Aldrich)
Vasculogenic differentiation medium (VDM)	From EGM-2 MV BulletKit (Lonza)[a]: Endothelial Basal Cell Medium-2 + 5% FBS hFGF-β R^3-IGF-1 VEGF Ascorbate
Dual-differentiation medium (DDM)	50:50 mixture of ODM and VDM

[a]Lonza BulletKit includes standard proprietary concentrations of listed substrates.

DMEM, Dulbecco's modified Eagle's media; FBS, fetal bovine serum; EGM, endothelial growth medium; hFGF, human fibroblast growth factor; IGF, insulin-like growth factor; VEGF, vascular endothelial growth factor.

Carlsbad, CA) and filtered. The tissue was digested using 1% collagenase at 37°C for 90 min. After centrifugation (1300 rpm for 10 min), the oily supernatant was removed, and the remaining cell suspension was incubated with sterile ammonium chloride at 37°C for 30 min. The mononuclear cell layer was isolated by density gradient centrifugation using Histopaque-1077 (Sigma-Aldrich, St. Louis, MO). Isolated cells were seeded on polystyrene plates at a density of 1×10^3 cells/cm^2 in the stem cell growth medium to encourage adherence.[34] After 4 days, nonadherent cells were removed, and the stem cell expansion medium was used. Upon reaching 90% confluence, cells were passaged with 0.25% trypsin/0.1% EDTA (Lonza) and expanded until passage 3 with the stem cell expansion medium, whereupon they were termed ASCs and used in subsequent experiments. Normal human osteoblasts (NHOsts) (Lonza/Clonetics, Basel, Switzerland) and human umbilical vein ECs (HUVECs) (Lonza/Clonetics) were cultured in ODM and VDM, respectively.

Osteogenic differentiation and vasculogenic differentiation

ASCs were cultured in ODM or VDM to yield OPECs and EPECs, respectively. For some experiments, ASCs were differentiated in a 50:50 mixture of ODM:VDM termed dual-differentiation media (DDM). Cells were harvested at 3, 6, 9, 12, or 15 days of differentiation for further experiments.

Fluorescent labeling and coculture of EPECs and OPECs

EPECs and OPECs were differentiated as described above for 15 days. OPECs were stained with 3-3′-dioctadecyloxacarbocyanine perchlorate (diO), EPECs with 1,1′-dioctadecyl-3,3,3′,3′-tetramethylindodicarbocyanine-4-chlorobenzenesulfonate (diD), and HUVECs with 1,1′-dioctadecyl-3,3,3′3′-tetramethylindocarbocyanine perchlorate (diI) (Invitrogen/Molecular Probes, Carlsbad, CA), for 12 min at 37°C, and then washed in phosphate-buffered saline (PBS). Labeled OPECs, EPECs, and HUVECs were trypsinized and centrifuged at 1300 rpm for 10 min at 37°C, the supernatant was removed, and cells were resuspended in a medium. Subsequently, a 50:50 ratio of OPECs:EPECs was seeded onto polystyrene plates and cultured in DDM. At day 15, imaging was performed (20×) with an Eclipse TE300 inverted fluoroscope (Nikon, Melville, NY), using a rhodamine filter for diD and diI (*red*), and a fluorescein isothiocyanate filter for diO (*green*). Spot Software 4.1.1 (Diagnostic Instruments, Sterling Heights, MI) was used for image processing. Labeled HUVECs were plated alone or in a 50:50 ratio with labeled OPECs according to the Matrigel tubularization assay protocol described below.

Quantitative real-time polymerase chain reaction

For quantitative real-time polymerase chain reaction (qRT-PCR) experiments, total RNA was isolated from the processed lipoaspirate cells at each time point using the RNeasy Mini Kit and the RNase-Free DNase Kit (Qiagen, Germantown, MD). The RNA purity and concentration was evaluated with a NanoDrop 1000 spectrophotometer (Thermo Scientific, Waltham, MA). Concentrations of total RNA were equalized before reverse transcription with the Quantitect Reverse Transcription Kit (Qiagen). 18s rRNA was utilized as the normalizer gene. Primers were designed to span an intron whenever possible (Table 2). Oligonucleotide sets are of original design, except for *BGLAP* (osteocalcin),[35] *SPARC* (osteonectin),[36] *SPP1* (osteopontin),[37] and *SP7* (osterix).[38] All samples were run in triplicate using the Quantitect SYBR Green PCR Kit (Qiagen) with a DNA Engine Opticon 2 thermal cycler (Bio-Rad, Hercules, CA). Conditions were 95°C for 15 min, followed by 35 cycles of 94°C for 15 s, 53°C for 30 s, and 72°C for 30 s. Each set of primers was used to amplify a standard template series of pooled sample cDNA spanning a 1000-fold concentration range, and all sets of primers had an efficiency of greater than 90%, and a precision of $r^2 \geq 0.97$. Amplicon size and purity were confirmed with melting curves, and an H_2O negative control was run with each plate.

Fluorescence-activated cell sorting (FACS)

Cells cultured in ODM or VDM were trypsinized and washed in HBSS. About 1×10^5 cells were then blocked in 10% goat serum (Gibco) with PBS for 30 min and stained at 4°C for 45 min with relevant mouse anti-human antibodies:

Table 2. Polymerase Chain Reaction Primer Sequences

Gene	*Location*	*GeneID*	*Sense sequence (5′–3′)*	*Antisense sequence (5′–3′)*	*Size (bp)*
PECAM1	17q23	5175	TCATTGCTCTCTTGATCATTGC	AGCTTCCATATTGGGATCTGAC	115
CD34	1q32.2	947	ACTCCAGAGACAACCTTGAAGC	CAGCTGGAGGTCTTATTTTGCT	212
ENG	9q33-q34.1	2022	ATACCACTAGCCAGGTCTCGAA	TTTACACTGAGGACCAGAAGCA	175
MSX2	5q34-q35	4488	TCGGAAAATTCAGAAGATGGAG	TGGAGAGGTACTGTTTCTGACG	190
BGLAP	1q25-q31	632	ATGAGAGCCCTCACACTCCTC	GCCGTAGAAGCGCCGATAGGC	294
SPARC	5q31.3-q32	6678	GGCTCAAGAACGTCCTGGT	CTGCTTGATGCCGAAGCAG	374
SPP1	4q21-q25	6696	AGTACCCTGATGCTACAGACG	CAACCAGCATATCTTCATGGC	321
SP7	12q13.13	121340	GCCAGAAGCTGTGAAACCTC	GCTGCAAGCTCTCCATAACC	161
RUNX2	6p21	860	CCTTGACCATAACCGTCTTCA	GAGGCGGTCAGAGAACAAAC	146
SOX9	17q24.3-q25.1	6662	GACTCGCCACACTCCTCCT	AGGTCTCGATGTTGGAGATGA	238
FLT1	13q12	2321	TACTTGGATTTTACTGCGGACA	TCTAAAGTGGTGGAACTGCTGA	282
KDR	4q11-q12	3791	TCATCCTTACCAATCCCATTTC	ACTGGTAGGAATCCACAGGAGA	117
18s rRNA	Multiple sites	100008588	CATTCGAACGTCTGCCCTAT	GCCTTCCTTGGATGTGGTAG	131

allophycocyanin-conjugated anti-ENG (*CD105*), FITC-conjugated anti-*CD34*, phycoerythrin-conjugated anti-*PECAM1* (*CD31*), and phycoerythrin-conjugated anti-*BGLAP* (osteocalcin) (BD Biosciences, San Jose, CA/Miltenyi Biotec, Bergisch Gladbach, Germany). Staining for *FLT1* (*VEGFR1*) and *KDR* (*VEGFR2*) was performed using the monoclonal mouse anti-human VEGF-R PE sampler kit (R&D Systems, Minneapolis, MN). Cells were costained with 7-aminoactinomycin D (Invitrogen) to detect nonviable cells. Positive staining was measured using a FACSCaliber flow cytometer (BD Biosciences), and analyses were performed with FlowJo 8.0 software (TreeStar, Ashland, OR). NHOsts and HUVECs served as representative controls for terminally differentiated osteoblastic and ECs, respectively.

von Kossa mineralization assay

ASCs, EPECs, OPECs, HUVECs, and NHOsts were plated in triplicate wells at a density of 100,000 cells/well (50,000 of each cell type in coculture) and incubated at 37°C in appropriate media for 3 days (stem cell growth medium, VDM, ODM, VDM, and ODM, respectively). The mineralization medium was used for 18 additional days, and it is comprised of the DMEM with 10% FBS, 20 mM ascorbate, and 10 mM β-glycerophosphate (Sigma-Aldrich). Twenty-one days after initial plating, cells were fixed in methanol at −20°C for 2 min and subsequently exposed to 2% silver nitrate for 1 h under a 50-watt lamp. Representative polarized-light photomicrographs of low-power fields (LPF, 4×) were taken. Bone nodules were counted by computer-aided image analysis,[39] using the object counting function in NIS-Elements v3.0 BR software (Nikon), excluding objects with areas $<70\,\mu m^2$. This area was chosen to exclude cellular debris and include nearly all bone nodules: the average bone nodule size of bone cells plated for 21 days were reported to be $\sim 96 \pm 21\,\mu m^2$.[39] The bone nodule number and area were measured and recorded in triplicate randomly selected areas within each well.

Matrigel tubularization assay

The Matrigel basement membrane matrix (BD Biosciences) was thawed on ice and incubated at room temperature for 60 min. 50,000 cells of a given type (25,000 of each cell type in coculture) were plated onto the matrix in triplicate wells, and incubated at 37°C, 5% CO_2, 95% humidified air for up to 28 h. A blinded investigator selected three random LPFs after 6- and 24-h incubation periods and recorded light photomicrographs (4×). Intact complete microtubules completely enclosed and visible within each field were counted manually. Microtubules were also examined under fluorescent microscopy (10×) 28 h after seeding (Nikon Eclipse TE 300).

Osteogenic-to-vasculogenic redirection

A redirection experiment was performed to assess the potential for ASCs to reverse lineage commission during osteogenic differentiation. After OPECs were cultured in ODM for 3, 6, 9, 12, or 15 days, the medium was aspirated and cells were washed once in PBS (Sigma-Aldrich). The OPECs were then cultured in VDM for a total of 15 days. These redirected cells were then subjected to the Matrigel tubularization assay as described above.

Statistical analysis

Relative quantification of RNA expression compared to ASCs using qRT-PCR was calculated in terms of fold change using the ΔΔCt method, with error bars graphed as ±1 standard deviation. Bone nodule and microtubule counts from triplicate random LPFs are reported as mean ± 1 standard error of the mean. Data from the qRT-PCR, von Kossa, and tubularization assays were analyzed with the unpaired two-tailed Student's *t*-test. Statistical significance was set at $p < 0.05$. Since we expect, but cannot necessarily assume, a Gaussian distribution for RNA data, the Kruskal–Wallis and the Mann–Whitney U tests (one-tailed *p*-value) were also performed for selected qRT-PCR data, whenever we noted a statistically significant difference in expression (data not shown). The above nonparametric tests ($p \leq 0.05$) confirmed the validity of our conclusions from qRT-PCR data presented in this work using the unpaired two-tailed Student's *t*-test.

Results

Coculture suitability for vascularized bone engineering

We tested eight coculture combinations for growth compatibility, along with ASCs in monoculture (Fig. 1A). Each of the coculture combinations had unrestricted growth of vascular and osteogenic cell types when cultured in DDM (50:50 ODM:VDM combination media) (data not shown). We found ASCs cultured for 15 days in DDM have the capacity to form microtubules or bone nodules (Fig. 1B: Top, Bottom), suggesting some retention of pluripotency. In addition, we observed that fluorescently labeled 15-day predifferentiated osteogenic (e.g., OPECs) and vasculogenic (e.g., EPECs) cells grew in multiple adjacent or overlapping multiplanar cellular networks when cocultured in DDM for an additional 15 days (Fig. 1C). These findings provide evidence that our tested cell types are compatible and suitable for vascularized bone engineering.

FIG. 2. Limited stem cell marker expression of dual-differentiated ASCs. **(A)** ASCs differentiated in DDM for 15 days did not produce significant upregulation of osteogenic or vasculogenic end-differentiation markers, *PECAM1* (*CD31*) and *SPP1* (osteopontin), as measured by quantitative real-time polymerase chain reaction (qRT-PCR). ASCs, 15-day EPECs, and 15-day OPECs are used as comparative controls. Asterisks mark statistically significant upregulation of the given gene compared to all three other cell types ($p < 0.05$). **(B)** ASCs were isolated from human lipoaspirate and grown in vasculogenic or osteogenic induction media for 15 days to yield populations of EPECs and OPECs, respectively. qRT-PCR was performed to measure the relative expression levels of *ENG* (*CD105*), *SOX9*, and *RUNX2* at several time points in a 15-day differentiation course. Normal human osteoblast (NHOst) and human umbilical vein ECs (HUVECs) were used to represent terminally differentiated OB and ECs, indicated by time point ∞, and expression levels were normalized relative to ASCs. Additionally, fluorescence-activated cell sorting (FACS) was performed on selected cell populations to measure the proportion of cells expressing *ENG*.

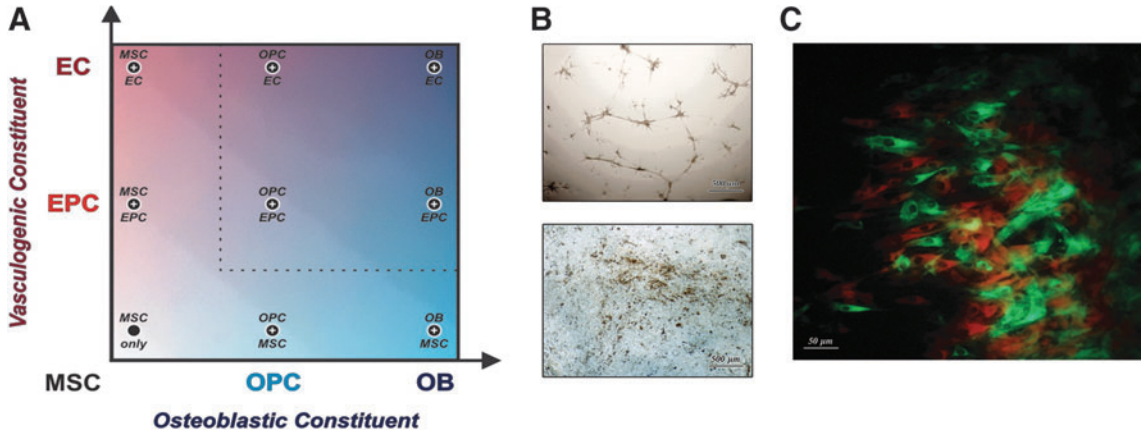

FIG. 1. Many coculture combinations are possible for bone engineering. **(A)** Many cell types from a variety of tissue sources can be utilized for vascularized bone tissue engineering. These cells can range from undifferentiated mesenchymal stem cells (MSC) to well-differentiated osteoblasts (OB) and endothelial cells (EC), via osteoprogenitor cells (OPC) and endothelioprogenitor cells, respectively. We used adipose-derived stem cells (ASC) to yield osteoprogenitor-rich endothelioprogenitor-rich cell populations (OPECs and EPECs, respectively). **(B)** ASCs cultured in 50:50 mixture of osteogenic differentiation medium (ODM):vasculogenic differentiation medium (VDM) media (i.e., dual-differentiation media [DDM]) were found to yield microtubules (top) or bone nodules (bottom) when subjected to the Matrigel tubularization assay or von Kossa assay, respectively. Representative light micrographs are shown (4×). **(C)** Predifferentiated OPECs and EPECs grew in multiple adjacent or overlapping multiplanar cellular networks. These OPECs and EPECs were then labeled with fluorescent markers OPECs (3-3′-dioctadecyloxacarbocyanine perchlorate [diO], green) and EPECs (1,1′-dioctadecyl-3,3,3′,3′-tetramethylindodicarbocyanine-4-chlorobenzenesulfonate, red), respectively, and cocultured in DDM for 15 days. The fluorescent photomicrograph demonstrates successful coculture of these two cell populations in direct contact (20×).

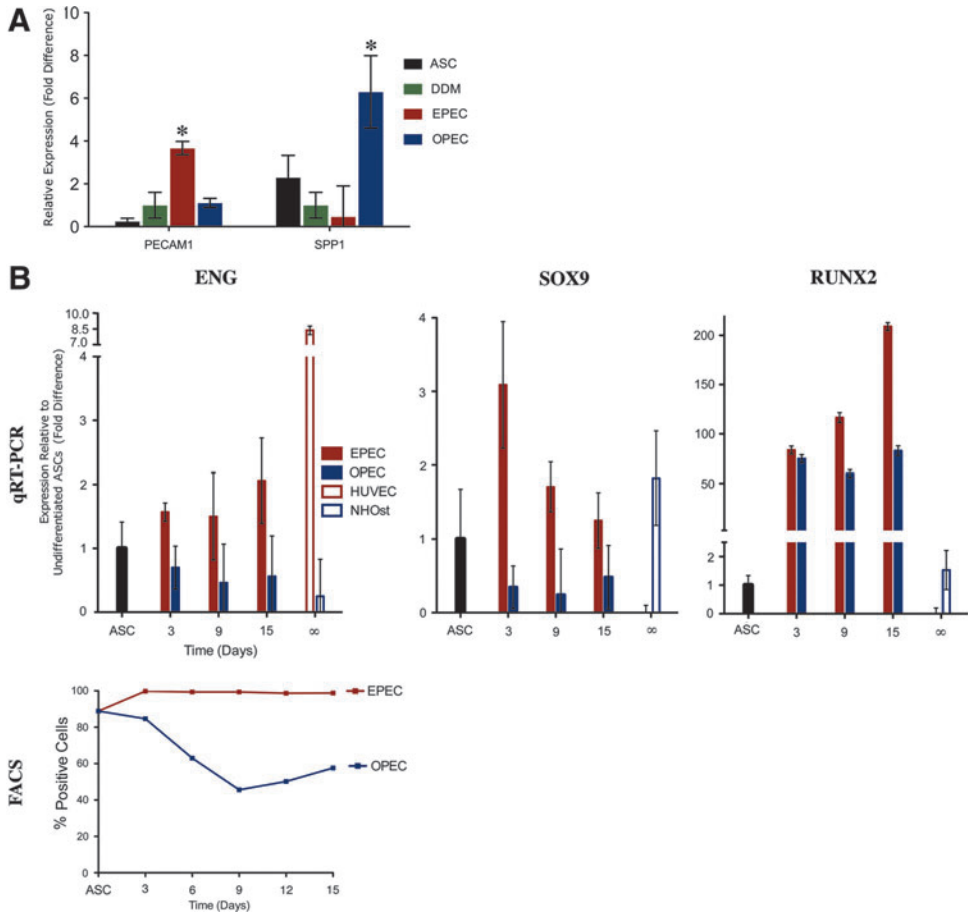

Table 3. Markers of Differentiation

Osteoblastic phenotype	*Biological markers*[26,27,46,47,50–53]
MSC	*RUNX2, SOX9, ENG*
OPC	*RUNX2, MSX2, TWIST1, TWIST2 (SOX9* disappears)
Pre-Ob	*RUNX2, SP7, SPP1, ATF4*
Ob	*RUNX2, SP7, SPP1, BGLAP, SPARC, ALPL*
Osteocyte	*PHEX, DMP1, SPP1, BGLAP(RUNX2* inhibits osteocyte formation)
Endothelial phenotype	*Biological markers*[46,54–56]
MSC	*RUNX2, SOX9, ENG*
EPC	*ENG, CD34, FLT1, KDR*
EC	*ENG, PECAM1*

MSC, mesenchymal stem cell; OPC, osteoprogenitor cell; Ob, osteoblast; EPC, endothelial progenitor cell; EC, endothelial cell. Gene names follow the HUGO gene nomenclature committee recommendations.

Limitations in the duality of ASC-derived osteogenic and vasculogenic populations

In light of the above findings, we differentiated ASCs in DDM for 15 days and measured the expression of vascular and osteogenic end-differentiation markers (*PECAM1* and *SPP1*, respectively), and compared their expression to EPECs and OPECs differentiated for 15 days (Fig. 2A). We found that ASCs differentiated in DDM did not upregulate these markers to a significant degree, remaining at levels not significantly different from those seen in control undifferentiated ASCs. By comparison, EPECs demonstrated significantly increased expression of *PECAM1* (3.67-fold ± 0.311 $p < 0.017$) and OPECs showed significantly increased expression of *SPP1* (6.30-fold ± 1.69 $p < 0.042$), as expected.

As the above vascular and bone end-differentiation markers were not expressed robustly in DDM-cultured ASCs, we next investigated ASC populations differentiated into vasculogenic and osteogenic lineages in VDM or ODM separately (i.e., EPECs and OPECs, respectively). Expression levels of several MSC markers were compared (Table 3). In addition, HUVECs and NHOst cells were used as differentiated comparative controls (Fig. 2B). Transcription of *ENG*

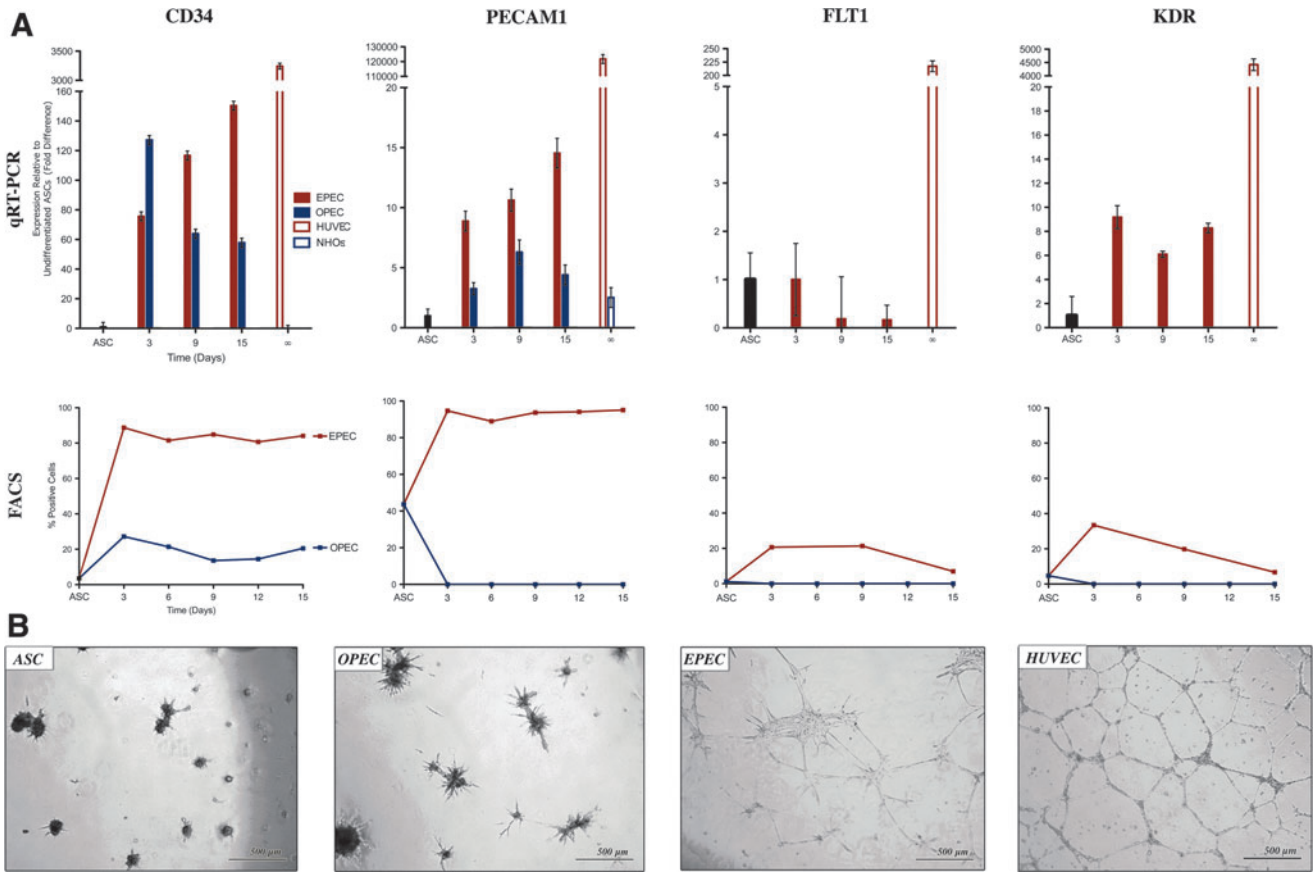

FIG. 3. Ontogeny of ASC-derived population commitment to the vascular lineage. **(A)** qRT-PCR and FACS were performed to measure the relative expression level of various vasculogenic markers in EPECs at several time points in a 15-day differentiation course. NHOsts and HUVECs were used to represent terminally differentiated OB and ECs, indicated by time point ∞, and expression levels were normalized relative to ASCs. **(B)** The Matrigel assay was used to assess the capacity of ASCs for microtubule formation. Fresh ASCs and OPECs at all time points (day 3 shown) were unable to form microtubules (4×). EPECs demonstrated tubularization capacity at all time points measured (day 3 shown). HUVECs are shown as a positive control.

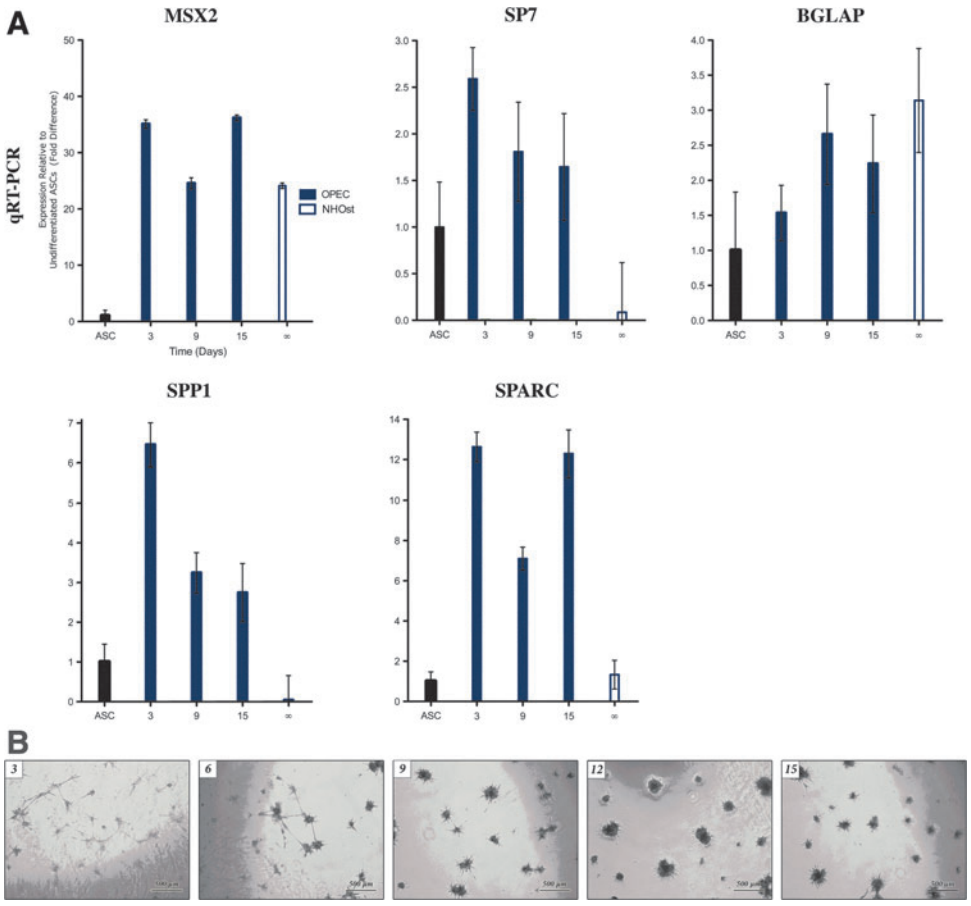

FIG. 4. Ontogeny of ASC-derived population commitment to the bone lineage. **(A)** qRT-PCR was performed to measure the relative expression level of various osteogenic markers in OPECs at several time points in a 15-day differentiation course. NHOst cells were used to represent terminally differentiated OB, indicated by time point ∞, and expression levels were normalized relative to ASCs. **(B)** Redirection capacity of OPECs to the vasculogenic lineage. OPECs underwent varying durations of osteogenic differentiation in ODM (days numbered), were subsequently cultured in VDM for 14 days, and then subjected to the Matrigel assay. OPECs redirected only at the earliest stages of osteogenic differentiation (3 and 6 days) demonstrated the capacity for microtubule formation (4×). OPECs could not be redirected to produce microtubules at 9, 12, and 15 days, suggesting commission to the osteogenic lineage occurs between days 6 and 9.

in EPECs was shown by qRT-PCR to trend up 2.0-fold by day 15 ($p = 0.08$), but ENG was shown by fluorescence-activated cell sorting (FACS) to be expressed in 99% of all cells by day 3. OPECs had an insignificant decrease in *ENG* expression relative to ASCs ($p = 0.42$ at day 15). *SOX9* mRNA was downregulated throughout the osteogenic induction by an insignificant amount ($p \geq 0.20$). Interestingly, *SOX9* was significantly upregulated 3.1-fold at day 3 of the vasculogenic induction ($p < 0.05$), gradually decreasing to essentially the same level seen in fresh ASCs by day 15 ($p = 0.60$). *RUNX2* was significantly upregulated at day 3 of ODM culture, to 75-fold the expression level seen in fresh ASCs ($p < 0.01$). Interestingly, expression of *RUNX2* was regulated to an even higher extent in ASCs cultured in VDM (209-fold at day 15).

The ontogeny of ASC commitment to EPECs

Three hallmark vasculogenic markers, *CD34*, *PECAM1*, and *KDR* (Table 3), were expressed and significantly upregulated in EPECs throughout vasculogenic commitment ($p < 0.01$) (Fig. 3A). By day 15 of vasculogenic differentiation, transcriptional expression of *CD34* increased 150-fold and *PECAM1* increased 14.5-fold relative to ASCs ($p < 0.01$). In contrast, OPECs had only a brief, dramatic increase in *CD34* by 127-fold at day 3 ($p < 0.01$). *KDR* was significantly

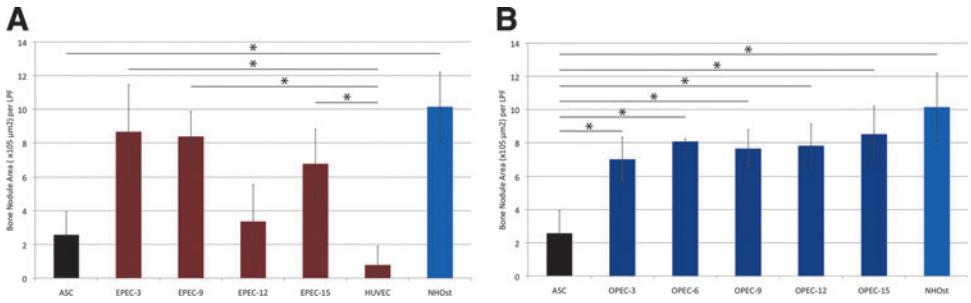

FIG. 5. Versatility of ASCs. Bone nodule formation capacity (nodule area) of EPECs **(A)**, and OPECs **(B)**, at several time points in a 15-day differentiation course are compared that to ASCs, NHOsts, and HUVECs. Numbers following the cell type indicate number of days the cell type was subjected to appropriate differentiation media. Asterisks indicate statistical significance ($p < 0.05$).

FIG. 6. OPECs cocultured with HUVECs yield robust mineralization capacity. **(A)** The von Kossa assay was performed to assess mineralization and bone-nodule formation capacity of various cell types, individually and in coculture. OPECs and EPECs underwent a 15-day differentiation course. Representative photomicrographs are shown for various cell cultures in monoculture and coculture (4×). Cocultured EPECs/OPECs produced sparse bone nodules in an uneven distribution. EPECs/NHOsts produced a density of nodules similar to those by NHOsts. Surprisingly, ASCs/HUVECs and OPECs/HUVECs generated abundant bone nodules, more than monocultures of each cell type individually. **(B)** Bone nodule formation was quantified with light microscopy by the nodule area (μm^2), **(C)** and bone nodule number, in triplicate low-power fields (LPFs) (4×). The nodule number and nodule area (μm^2) per LPF were examined. Single and double asterisks indicate statistical significance ($p < 0.05$ and $p < 0.01$, respectively).

upregulated in EPECs between 6.1-9.2-fold from days 3–15 in VDM ($p < 0.01$). FACS analysis showed that 4% and 44% of ASCs expressed *CD34* and *PECAM1*, respectively. *CD34* expression increased to 84% throughout vasculogenic commitment. In contrast, *CD34* expression in OPECs peaked at day 3 (27%), and then dropped (14%) by day 9. FACS also showed *PECAM1* was persistently expressed in 95% of EPECs throughout vasculogenic differentiation. Paradoxically, transcriptional expression of *PECAM1* was moderately elevated throughout the osteogenic induction, peaking at 6.3-fold on day 9 ($p < 0.01$). However, this did not surpass the significantly higher level of *PECAM1* expression during vasculogenic commitment, 14-fold ($p < 0.01$). FACS showed that *FLT1* and *KDR* were expressed on ~20%–35% of cells during days 3 and 9 of the vasculogenic differentiation, and expression of both markers subsequently dropped to levels comparable to undifferentiated ASCs by day 15. *FLT1* was downregulated throughout the vasculogenic course, decreasing 6.0-fold by day 15, but this change was not statistically significant ($p = 0.09$).

As expected Matrigel assays demonstrated HUVECs robust capacity to tubularize (94 ± 11.6 per LPF). Undifferentiated ASCs did not have the ability to form microtubules, nor did OPECs at any time point (Fig. 3B). However, EPECs demonstrated tubularization capacity beginning at 3 days (27 ± 4.4 per LPF) and at all subsequent time points.

The ontogeny of ASC commitment to OPECs

Key early and late osteogenic differentiation markers were measured in OPECs (Table 3). *MSX2* was significantly upregulated 25-to-36-fold throughout osteogenic induction ($p < 0.01$) (Fig. 4A). *SP7* was upregulated in OPECs by 2.6-fold at day 3 ($p < 0.05$). *BGLAP* expression in OPECs trended up between days 3 and 15, but was not significantly elevated compared to ASCs ($p > 0.05$ at each time point). Expression in NHOst cells was not significantly different from that seen at day 15 of the osteogenic induction course ($p = 0.20$), but was significantly greater than that seen in ASCs ($p < 0.05$). *BGLAP* expression was present in ~3%–6% of OPECs at all measured time points. *SPP1* was significantly upregulated 6.5-fold in OPECs at day 3 ($p < 0.01$). Expression subsequently declined to 2.7-fold by day 15. *SPARC* expression in OPECs was significantly upregulated 12.4-fold compared to ASCs at days 3 and 15, with a transient decrease at day 9 ($p < 0.01$ at each time point). NHOst cells expressed *SPARC* at the same level as ASCs did.

ASCs were cultured in ODM for varying lengths of time up to 15 days, abruptly switched to VDM for 14 days, and then subjected to the Matrigel assay (Fig. 4B). ASCs had the potential to form microtubules if redirected from ODM to VDM at any measured time point before day 9. However, if ASCs were redirected at 9 days or later, these cells had lost their capacity to form microtubules.

Comparative analysis of bone nodule formation in coculture combinations

We were not surprised to find that undifferentiated ASCs formed significantly fewer bone nodules than NHOsts ($p = 0.018$) (Fig. 5A). Surprisingly, EPECs demonstrated the capacity to form bone nodules at nearly all levels of differentiation ($p < 0.05$). By 15 days of differentiation, there was no significant difference in bone nodule formation of EPECs and NHOsts ($p = 0.334$). In contrast, OPECs consistently showed a significant increase in bone nodule formation from day 3 to 15 of differentiation compared to ASCs ($p < 0.05$ at all time points) (Fig. 5B).

Building on the above findings, we cocultured eight cell-type combinations and compared their bone nodule formation capacity (Fig. 6). The greatest numbers of bone nodules were consistently produced by the two coculture combinations that include a less differentiated osteoblastic cell and a fully differentiated EC: the OPEC/HUVEC and ASC/HUVEC (366 ± 51.9 and 399 ± 79 nodules per LPF, respectively) (Fig. 6B, C). These combinations produced a significantly greater number of bone nodules, with larger areas, when compared to NHOsts or OPECs in monoculture ($p < 0.05$).

Comparative analysis of microtubule formation in coculture combinations

HUVECs in monoculture demonstrated the greatest number of microtubules formed at 6 (81.2 ± 4.99 tubules per LPF) and 24 h (32.0 ± 7.55 tubules per LPF) (Fig. 7A). Compared to HUVECs alone, cocultured OPECs/HUVECs had a capacity for microtubule formation that trended

FIG. 7. OPECs cocultured with HUVECs yield robust microtubule formation. **(A)** Microtubule formation by monocultures and cocultures at 6 h (Top) and 24 h (Bottom) using the Matrigel assay. Tubules were counted only if completely enclosed and completely in view under light microscopy (4×). Results reported as average number of tubules per triplicate LPF. Single and double asterisks indicate statistical significance ($p < 0.05$ and $p < 0.01$, respectively). **(B)** Light microscopy images (4×) of microtubule formation by HUVECs and cocultured OPECs/HUVECs at 6 h postseeding, and fluoroscopic images (10×) of 1,1′-dioctadecyl-3,3,3′3′-tetramethylindocarbocyanine perchlorate-labeled HUVECs alone (red), or cocultured with diO-labeled OPECs (green), at 28 h postseeding.

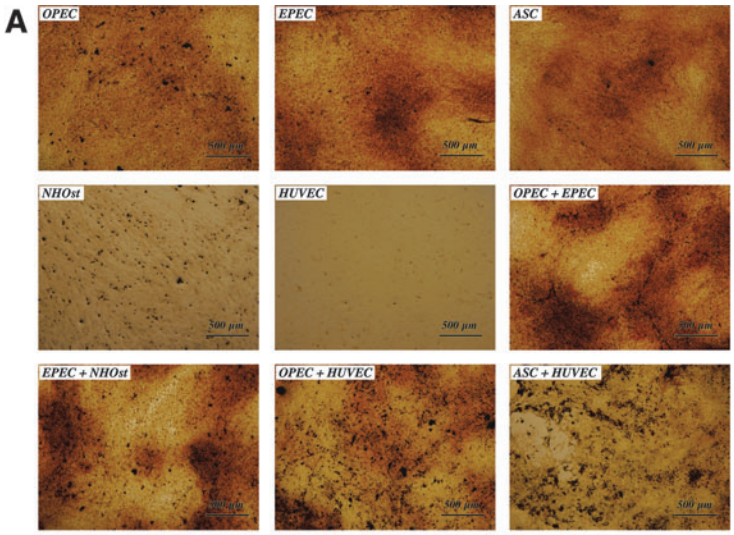

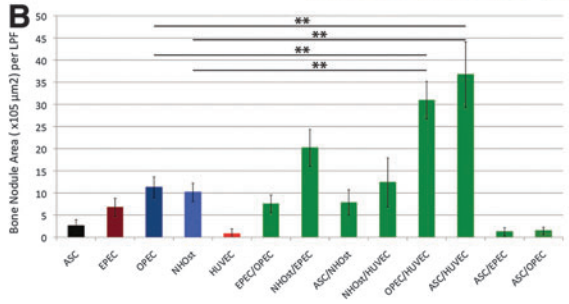

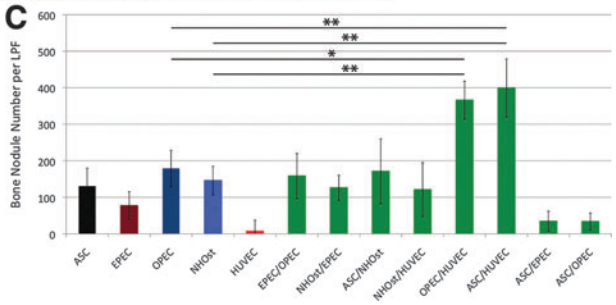

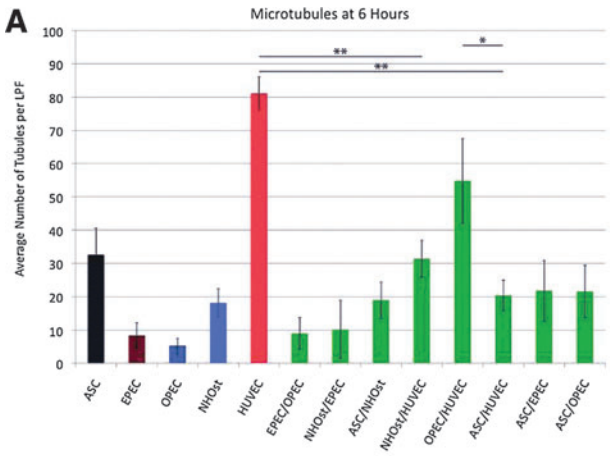

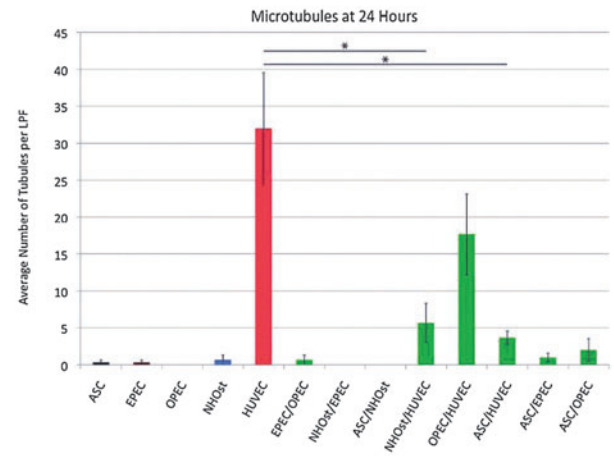

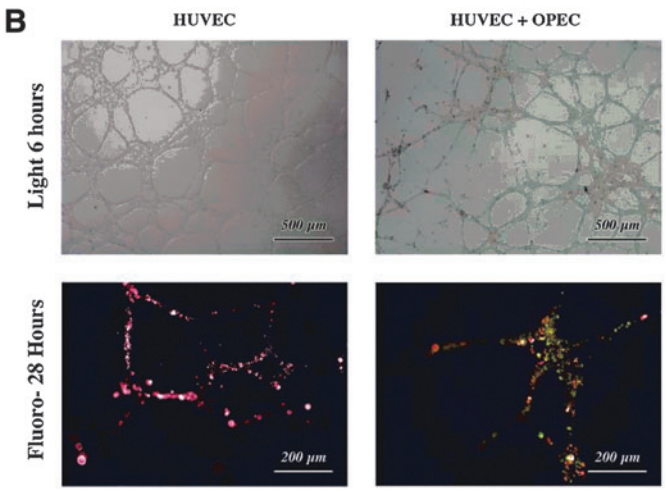

lower, but was not statistically different (54.8 ± 12.7 tubules per LPF at 6 h, $p = 0.090$; 17.6 ± 5.48 tubules per LPF at 24 h, $p = 0.199$). In contrast, all other tested coculture combinations had significantly less microtubule formation compared to HUVECs in monoculture at 24 h ($p < 0.05$ for all groups).

In addition to forming the greatest number of tubules in coculture, the morphology of microtubules produced by cocultured OPECs/HUVECs was most similar to that of HUVECs in monoculture (Fig. 7B). Interestingly, Matrigel assays of fluorescently tagged HUVECs and OPECs cocultured for 28 h demonstrated the presence of both cell types within the tubules. The significance of this finding remains unknown.

Discussion

For over half a billion years, tissue development and repair mechanisms have been shaped by respiratory constraints.[40] However, when stromal cells are studied in monoculture, the respiratory constraints of *de novo* tissue formation remained obscured. While recent work has suggested that osteoblastic stromal cells enhance EC function by producing matrix molecules (e.g., *SPP1*) and angiogenic signals (e.g., *VEGFA*),[41,42] our findings indicate that the relationship is bidirectional. This new finding seems logical considering the elemental respiratory requirements of nascent bone. Interestingly, we found that the bidirectional relationship is influenced by the degree of differentiation of either cellular constituent.

We initially found that ASCs cultured in 50:50 mixture of ODM:VDM media (i.e., DDM) promisingly yielded microtubules and bone nodules when subjected to the Matrigel assay or von Kossa assay, respectively. However, this medium did not produce any significant upregulation of representative endothelial or osteogenic end-differentiation markers after 15 days (*PECAM1* and *SPP1*, respectively). Thus, although this simple osteogenic/vasculogenic medium mixture may yield the two basic end-differentiation phenotypes when they are studied in isolation, this medium is unlikely to lead to the expression of the set of extracellular proteins and receptors involved in cell–cell communication that would be necessary for robust composite bone tissue formation. We believe this would be due to the absence of a combination of lineage-specific progenitor cells in direct contact and, consequently, the absence of communication among them.

Thus, it is tempting to speculate that two differentiated cell types (e.g., HUVECs and NHOst) or two progenitor cell types (e.g., EPECs and OPECs) function cooperatively to create vascularized bony tissue—especially since we found fluorescently tagged EPECs and OPECs coexist stably in coculture. However, when NHOsts were cultured with HUVECs, or when EPECs and OPECs were cocultured, resultant microtubule formation was consistently underwhelming. On the other hand, when OPECs were cultured with HUVECs, the greatest numbers of microtubules were formed of all the coculture combinations tested. The notion that an OPEC rather than an NHOst cooperatively interacts with a HUVEC may seem trivial at a glance. However, the OPEC/HUVEC combination allows for a unified view of the multiplicity of coculture candidates. Since OPECs are a heterogeneous population of cells that include adventitial stromal cells, pre-OB, and adipocytes,[27] all niche effects could be seen as rooted in the pivotal role of a single cell type (here, the HUVEC) acting as a dynamic organizer of a complex system of effector cells, conveying diversified instructive cues to developing vascularized bone tissue. This bidirectional yet hierarchical interaction is suggested by our observation that cocultured HUVEC and OPEC populations were found by fluorescence microscopy to be incorporated into resultant microtubules.

How immature osteoblastic cells improve or stabilize tubule formation remains to be elucidated, but this phenomenon may result from OPECs stimulating primary microtubule formation, and/or by stabilizing tubules that have already formed. Perhaps, prostaglandins, such as PGE2, contribute to this effect, as they have been shown to have profound effects on bone fracture healing, osteoclastogenesis, and osteoblastic differentiation.[43] Data from our experiments suggest that both mechanisms are active. For example, we found that *SPARC* is significantly upregulated in OPECs, and downregulated in NHOsts as well as in ASCs. This multifunctional glycoprotein has known important roles in angiogenesis and vascular homeostasis,[44] and may be responsible for the positive effect of OPECs on HUVEC-microtubules. Additionally, this effect may be, in part, mediated by *SPP1*—another protein we found expressed highly in OPECs and downregulated in NHOsts as well as ASCs: media with high concentration of SPP1 is known to increase HUVEC migration and induce tubularization.[45] If a similar interaction occurs between cocultured OPEC/HUVECs, it would explain why this combination yields a large number of microtubules, while ASC/HUVECs and NHOst/HUVECs do not.

As in microtubule formation, the beneficial effect of progenitor cell coculture on bone nodule formation was limited to combinations of immature osteoblastic cells with mature ECs: only OPEC/HUVEC and ASC/HUVEC combinations produced a significant enhancement in nodule formation. When OPECs were cultured in direct contact with HUVECs, bone nodule formation was significantly enhanced, compared to monocultures of OPECs or HUVECs. Thus, the angiogenic cell influence on osteogenic cell function was observed only when a more differentiated angiogenic cell (the HUVEC) was cultured in direct contact with a less differentiated osteoblastic cell (the OPEC or ASC).

Guillotin *et al.* recently made the observation that *RUNX2* is downregulated in human OPCs when cocultured with HUVECs,[25] which makes sense since *RUNX2* is known to inhibit osteocyte end-differentiation, despite playing an important role in early osteoblastogenesis.[46] Considering our finding that cocultured OPECs/HUVECs have a high capacity for bone nodule production, possible HUVEC-induced downregulation of *RUNX2* in OPCs may be a necessary mechanism by which HUVECs push OPECs to end-differentiate. Several approaches are currently being explored to elucidate this mechanism of communication, including coculture divided by a semipermeable membrane, or with gap junction inhibition.

During endochondral ossification, late chondrocyte differentiation promotes capillary sprouting and invasion into the hypertrophic cartilage.[9] *SOX9* is constitutively expressed

in MSCs and is upregulated during chondrogenesis, but downregulated during osteogenesis.[46,47] Concordantly, we demonstrated that *SOX9* expression was downregulated significantly by day 3 of OPEC differentiation. Considering its role in inhibiting osteogenesis, the presence of *SOX9* expression in NHOst cells is surprising. To our knowledge, only one other group has reported similar results, finding the presence of SOX9 in total protein lysates from adult mouse bone.[48] Interestingly, the increased expression of *SOX9* in EPECs at day 3 suggests chondrogenic potential in EPECs that disappears by day 9. This information may prove useful for experiments directed toward engineering cartilage itself, or for utilizing cartilage as an intermediate toward endochondral bone formation.

Our study is limited by several factors. First, there is a wide range in the age of adipose donor patients (ages 18–55). Although this range reflects the ages of patients commonly undergoing lipoaspiration, some phenotypic differences can be found when comparing the activity of bone marrow-derived MSCs from donors younger than 18 years and older than 50 years.[12] Future studies may benefit from a more restrictive age range. Second, the viability of engrafted bone is, in part, contingent on the distance of the stromal cell from its blood supply since oxygen and nutrient diffusion necessary to support tissue metabolism is limited to 200 μm.[49] Our experiments are 2D and, therefore, by their very nature, not subjected to the diffusional limitations governing the viability of 3D composite tissue. Yet, the phenotypic data yielded here still provide a rational basis for the selection of coculture combination in future 3D experiments. While it is tempting to speculate that the optimal cellular combinations in the Petri dish will prove equally advantageous in 3D, this remains to be proven. Our study is also limited by the decision to primarily present qRT-PCR/RNA data as a window into the up- and downregulation of the specific differentiation markers at hand, without confirmation by protein expression assays. However, the inclusion of protein assay data is not central to the drive of this work, given our purpose is to explore the plasticity and lineage commission of ASC-derived OPEC and EPEC populations to determine if optimal cell combinations exist for vascularized bone engineering, and was deferred for future studies involving the optimized cell combination that ultimately prevails as the standard in our field.

We found OPECs became increasingly lineage committed and lose the capacity for redirection to the vasculogenic lineage when exposed to ODM for 9 days or more, but retained redirection capacity with short-term exposure up to 6 days. Thus, irreversible commitment to the osteogenic lineage occurs at some point between 6 and 9 days of differentiation. Although we used 15-day-old OPECs in cocultures, 9 days of differentiation is likely sufficient to yield OPECs with osteogenic potential for use in future vascularized bone construct applications. Surprisingly, our data did not show a significant decrease in the bone nodule area as EPECs differentiated to day 15. This may suggest that through day 15, EPEC populations are either heterogeneous or still uncommitted to the endothelial pathway. However, redirection experiments to elucidate the timing of EPEC lineage redirection would be of little value, considering our findings suggest that the HUVEC is the most promising EC type for coculture.

Taken together, our results suggest that the OPEC/HUVEC is the most promising coculture combination for future experiments in vascularized bone engineering. While the prospect of vascularized bone synthesized entirely from endogenous ASCs is enticing and elegant, the OPEC/HUVEC combination is realistic and worthy of further study. This cell combination, if proved successful for bone construct applications, would ultimately require harvesting cells from adipose tissue and banked cord blood—a worthy goal, since our waistlines are ever-increasing and cord blood banking is ever more popular.

Conclusions

To create vascularized bone, one must develop methods for successful coculture of multiple cell types. Our results suggest that a combination of a less-differentiated osteoblastic cell with a differentiated EC (i.e., OPEC/HUVEC) is most promising for this purpose. Thus, our results reinforce the concept of predifferentiating the angiogenic cell type to develop a microvascular network, before the introduction of the stromal osteogenic cell. These findings bring us a step closer to defining the optimal cell combination and ideal coculture conditions for 3D vascularized bone engineering using ASC populations.

Acknowledgments

This work was supported, in part, by the 2007 Lyndon Peer Research Fellowship (A.C.A.), administered by the Plastic Surgery Educational Foundation (PSEF); the 2007 Bernd Spiessl Research Award (A.C.A.), administered by the American Society of Maxillofacial Surgery (ASMS) through the courtesy of Synthes CMF; the 2007 & 2008 PSEF Basic Science Research Grants (A.C.A.); the 2008 Alpha Omega Alpha (AΩA) Carolyn L. Kuckein Research Fellowship (A.M.S.); the 2010 AOCMF Award; and the 2008 Association of Academic Plastic Surgeons (AAPS) Academic Scholar Award (S.M.W.). We would also like to acknowledge the kind assistance of Dr. Yuexun Liu at the NYU College of Dentistry.

Disclosure Statement

No competing financial interests exist.

References

1. Cheng, M.H., Brey, E.M., Allori, A., Satterfield, W.C., Chang, D.W., Patrick, C.W., Jr., and Miller, M.J. Ovine model for engineering bone segments. Tissue Eng **11,** 214, 2005.
2. Bouletreau, P.J., Warren, S.M., Spector, J.A., Steinbrech, D.S., Mehrara, B.J., and Longaker, M.T. Factors in the fracture microenvironment induce primary osteoblast angiogenic cytokine production. Plast Reconstr Surg **110,** 139, 2002.
3. Eghbali-Fatourechi, G.Z., Lamsam, J., Fraser, D., Nagel, D., Riggs, B.L., and Khosla, S. Circulating osteoblast-lineage cells in humans. N Engl J Med **352,** 1959, 2005.
4. Galiano, R.D., Tepper, O.M., Pelo, C.R., Bhatt, K.A., Callaghan, M., Bastidas, N., Bunting, S., Steinmetz, H.G., and Gurtner, G.C. Topical vascular endothelial growth factor accelerates diabetic wound healing through increased angiogenesis and by mobilizing and recruiting bone marrow-derived cells. Am J Pathol **164,** 1935, 2004.

5. Tepper, O.M., Capla, J.M., Galiano, R.D., Ceradini, D.J., Callaghan, M.J., Kleinman, M.E., and Gurtner, G.C. Adult vasculogenesis occurs through *in situ* recruitment, proliferation, and tubulization of circulating bone marrow-derived cells. Blood **105,** 1068, 2005.
6. Park, S., Tepper, O.M., Galiano, R.D., Capla, J.M., Baharestani, S., Kleinman, M.E., Pelo, C.R., Levine, J.P., and Gurtner, G.C. Selective recruitment of endothelial progenitor cells to ischemic tissues with increased neovascularization. Plast Reconstr Surg **113,** 284, 2004.
7. Higashino, K., Viggeswarapu, M., Bargouti, M., Liu, H., Titus, L., and Boden, S.D. Stromal cell-derived factor-1 potentiates bone morphogenic protein-2 induced bone formation. Tissue Eng Part A **17,** 523, 2011.
8. Allori, A.C., Sailon, A.M., and Warren, S.M. Biological basis of bone formation, remodeling, and repair-part I: biochemical signaling molecules. Tissue Eng Part B Rev **14,** 259, 2008.
9. Allori, A.C., Sailon, A.M., and Warren, S.M. Biological basis of bone formation, remodeling, and repair-part II: extracellular matrix. Tissue Eng Part B Rev **14,** 275, 2008.
10. Allori, A.C., Sailon, A.M., Pan, J.H., and Warren, S.M. Biological basis of bone formation, remodeling, and repair-part III: biomechanical forces. Tissue Eng Part B Rev **14,** 285, 2008.
11. Gawlitta, D., Fledderus, J.O., van Rijen, M.H., Dokter, I., Alblas, J., Verhaar, M.C., and Dhert, W.J. Hypoxia impedes vasculogenesis of *in vitro* engineered bone. Tissue Eng Part A **18,** 208, 2012.
12. Pietilä, M., Palomäki, S., Lehtonen, S., Ritamo, I., Valmu, L., Nystedt, J., Laitinen, S., Leskelä, H.V., Sormunen, R., Pesälä, J., Nordström, K., Vepsäläinen, A., and Lehenkari, P. Mitochondrial function and energy metabolism in umbilical cord blood- and bone marrow-derived mesenchymal stem cells. Stem Cells Dev **21,** 575, 2012.
13. Yang, X.B., Whitaker, M.J., Sebald, W., Clarke, N., Howdle, S.M., Shakesheff, K.M., and Oreffo, R.O. Human osteoprogenitor bone formation using encapsulated bone morphogenetic protein 2 in porous polymer scaffolds. Tissue Eng **10,** 1037, 2004.
14. Jeon, O., Song, S.J., Kang, S.W., Putnam, A.J., and Kim, B.S. Enhancement of ectopic bone formation by bone morphogenetic protein-2 released from a heparin-conjugated poly(L-lactic-co-glycolic acid) scaffold. Biomaterials **28,** 2763, 2007.
15. Beloti, M.M., Sicchieri, L.G., de Oliviera, P.T., and Rosa, A.L. The influence of osteoblast differentiation stage on bone formation in autogenously implanted cell-based poly(lactide-co-glycolide) and calcium phosphate constructs. Tissue Eng Part A **18,** 999, 2012.
16. Kaigler, D., Wang, Z., Horger, K., Mooney, D.J., and Krebsbach, P.H. VEGF scaffolds enhance angiogenesis and bone regeneration in irradiated osseous defects. J Bone Miner Res **21,** 735, 2006.
17. Kanczler, J.M., Ginty, P.J., Barry, J.J., Clarke, N.M., Howdle, S.M., Shakesheff, K.M., and Oreffo, R.O. The effect of mesenchymal populations and vascular endothelial growth factor delivered from biodegradable polymer scaffolds on bone formation. Biomaterials **29,** 1892, 2008.
18. Singh, S., Wu, B.M., and Dunn, J.C. Accelerating vascularization in polycaprolactone scaffolds by endothelial progenitor cells. Tissue Eng Part A **17,** 1819, 2011.
19. Choong, C.S., Hutmacher, D.W., and Triffitt, J.T. Co-culture of bone marrow fibroblasts and endothelial cells on modified polycaprolactone substrates for enhanced potentials in bone tissue engineering. Tissue Eng **12,** 2521, 2006.
20. Jabbarzadeh, E., Starnes, T., Khan, Y.M., Jiang, T., Wirtel, A.J., Deng, M., Lv, Q., Nair, L.S., Doty, S.B., and Laurencin, C.T. Induction of angiogenesis in tissue-engineered scaffolds designed for bone repair: a combined gene therapy-cell transplantation approach. Proc Natl Acad Sci U S A **105,** 11099, 2008.
21. Hofmann, A., Ritz, U., Verrier, S., Eglin, D., Alini, M., Fuchs, S., Kirkpatrick, C.J., and Rommens, P.M. The effect of human osteoblasts on proliferation and neo-vessel formation of human umbilical vein endothelial cells in a long-term 3D co-culture on polyurethane scaffolds. Biomaterials **29,** 4217, 2008.
22. Duffy, G.P., Ahsan, T., O'Brien, T., Barry, F., and Nerem, R.M. Bone marrow-derived mesenchymal stem cells promote angiogenic processes in a time- and dose-dependent manner *in vitro.* Tissue Eng Part A **15,** 2459, 2009.
23. Koob, S., Torio-Padron, N., Stark, G.B., Hannig, C., Stankovic, Z., and Finkenzeller, G. Bone formation and neovascularization mediated by mesenchymal stem cells and endothelial cells in critical-sized calvarial defects. Tissue Eng Part A **17,** 311, 2011.
24. Rouwkema, J., Westerweel, P.E., de Boer, J., Verhaar, M.C., and van Blitterswijk, C.A. The use of endothelial progenitor cells for prevascularized bone tissue engineering. Tissue Eng Part A **15,** 2015, 2009.
25. Guillotin, B., Bareille, R., Bourget, C., Bordenave, L., and Amedee, J. Interaction between human umbilical vein endothelial cells and human osteoprogenitors triggers pleiotropic effect that may support osteoblastic function. Bone **42,** 1080, 2008.
26. Zuk, P.A., Zhu, M., Mizuno, H., Huang, J., Futrell, J.W., Katz, A.J., Benhaim, P., Lorenz, H.P., and Hedrick, M.H. Multilineage cells from human adipose tissue: implications for cell-based therapies. Tissue Eng **7,** 211, 2001.
27. Zuk, P.A., Zhu, M., Ashjian, P., De Ugarte, D.A., Huang, J.I., Mizuno, H., Alfonso, Z.C., Fraser, J.K., Benhaim, P., and Hedrick, M.H. Human adipose tissue is a source of multipotent stem cells. Mol Biol Cell **13,** 4279, 2002.
28. Planat-Benard, V., Silvestre, J.S., Cousin, B., Andre, M., Nibbelink, M., Tamarat, R., Clergue, M., Manneville, C., Saillan-Barreau, C., Duriez, M., Tedgui, A., Levy, B., Penicaud, L., and Casteilla, L. Plasticity of human adipose lineage cells toward endothelial cells: physiological and therapeutic perspectives. Circulation **109,** 656, 2004.
29. Halvorsen, Y.D., Franklin, D., Bond, A.L., Hitt, D.C., Auchter, C., Boskey, A.L., Paschalis, E.P., Wilkison, W.O., and Gimble, J.M. Extracellular matrix mineralization and osteoblast gene expression by human adipose tissue-derived stromal cells. Tissue Eng **7,** 729, 2001.
30. Erickson, G.R., Gimble, J.M., Franklin, D.M., Rice, H.E., Awad, H., and Guilak, F. Chondrogenic potential of adipose tissue-derived stromal cells *in vitro* and *in vivo*. Biochem Biophys Res Commun **290,** 763, 2002.
31. Toriyama, K., Kawaguchi, N., Kitoh, J., Tajima, R., Inou, K., Kitagawa, Y., and Torii, S. Endogenous adipocyte precursor cells for regenerative soft-tissue engineering. Tissue Eng **8,** 157, 2002.
32. Kolbe, M., Xiang, Z., Dohle, E., Tonak, M., Kirkpatrick, C.J., and Fuchs, S. Paracrine effects influenced by cell culture medium and consequences on microvessel-like structures in cocultures of mesenchymal stem cells and outgrowth endothelial cells. Tissue Eng Part A **17,** 2199, 2011.
33. Pu, L.L., Coleman, S.R., Cui, X., Ferguson, R.E., Jr., and Vasconez, H.C. Autologous fat grafts harvested and refined

by the Coleman technique: a comparative study. Plast Reconstr Surg **122,** 932, 2008.
34. Boquest, A.C., Shahdadfar, A., Brinchmann, J.E., and Collas, P. Isolation of stromal stem cells from human adipose tissue. Methods Mol Biol **325,** 35, 2006.
35. Diefenderfer, D.L., Osyczka, A.M., Garino, J.P., and Leboy, P.S. Regulation of BMP-induced transcription in cultured human bone marrow stromal cells. J Bone Joint Surg Am **85-A Suppl 3,** 19, 2003.
36. Jager, M., Fischer, J., Dohrn, W., Li, X., Ayers, D.C., Czibere, A., Prall, W.C., Lensing-Hohn, S., and Krauspe, R. Dexamethasone modulates BMP-2 effects on mesenchymal stem cells *in vitro*. J Orthop Res **26,** 1440, 2008.
37. Wongkhantee, S., Yongchaitrakul, T., and Pavasant, P. Mechanical stress induces osteopontin via ATP/P2Y1 in periodontal cells. J Dent Res **87,** 564, 2008.
38. Morsczeck, C. Gene expression of runx2, Osterix, c-fos, DLX-3, DLX-5, and MSX-2 in dental follicle cells during osteogenic differentiation *in vitro*. Calcif Tissue Int **78,** 98, 2006.
39. Nefussi, J.R., Ollivier, A., Oboeuf, M., and Forest, N. Rapid nodule evaluation computer-aided image analysis procedure for bone nodule quantification. Bone **20,** 5, 1997.
40. Baudouin-Cornu, P., and Thomas, D. Evolutionary biology: oxygen at life's boundaries. Nature **445,** 35, 2007.
41. Pacicca, D.M., Patel, N., Lee, C., Salisbury, K., Lehmann, W., Carvalho, R., Gerstenfeld, L.C., and Einhorn, T.A. Expression of angiogenic factors during distraction osteogenesis. Bone **33,** 889, 2003.
42. Mayer, H., Bertram, H., Lindenmaier, W., Korff, T., Weber, H., and Weich, H. Vascular endothelial growth factor (VEGF-A) expression in human mesenchymal stem cells: autocrine and paracrine role on osteoblastic and endothelial differentiation. J Cell Biochem **95,** 827, 2005.
43. Pountos, I., Georgouli, T., Calori, G.M., and Giannoudis, P.V. Do nonsteroidal anti-inflammatory drugs affect bone healing? a critical analysis. ScientificWorldJournal, 1, 2012 [Epub ahead of print]; DOI: 10.1100/2012/606404.
44. Brekken, R.A., and Sage, E.H. SPARC, a matricellular protein: at the crossroads of cell-matrix communication. Matrix Biol **19,** 816, 2001.
45. Takahashi, F., Akutagawa, S., Fukumoto, H., Tsukiyama, S., Ohe, Y., Takahashi, K., Fukuchi, Y., Saijo, N., and Nishio, K. Osteopontin induces angiogenesis of murine neuroblastoma cells in mice. Int J Cancer **98,** 707, 2002.
46. Marie, P.J. Transcription factors controlling osteoblastogenesis. Arch Biochem Biophys **473,** 98, 2008.
47. Karsenty, G., Kronenberg, H.M., and Settembre, C. Genetic control of bone formation. Annu Rev Cell Dev Biol **25,** 629, 2009.
48. Deshpande, A.M., Akunowicz, J.D., Reveles, X.T., Patel, B.B., Saria, E.A., Gorlick, R.G., Naylor, S.L., Leach, R.J., and Hansen, M.F. PHC3, a component of the hPRC-H complex, associates with E2F6 during G0 and is lost in osteosarcoma tumors. Oncogene **26,** 1714, 2007.
49. Sutherland, R.M., Sordat, B., Bamat, J., Gabbert, H., Bourrat, B., and Mueller-Klieser, W. Oxygenation and differentiation in multicellular spheroids of human colon carcinoma. Cancer Res **46,** 5320, 1986.
50. Malaval, L., Modrowski, D., Gupta, A.K., and Aubin, J.E. Cellular expression of bone-related proteins during *in vitro* osteogenesis in rat bone marrow stromal cell cultures. J Cell Physiol **158,** 555, 1994.
51. Chen, J., Singh, K., Mukherjee, B.B., and Sodek, J. Developmental expression of osteopontin (OPN) mRNA in rat tissues: evidence for a role for OPN in bone formation and resorption. Matrix **13,** 113, 1993.
52. Aubin, J.E. Advances in the osteoblast lineage. Biochem Cell Biol **76,** 899, 1998.
53. Yang, X., and Karsenty, G. ATF4, the osteoblast accumulation of which is determined post-translationally, can induce osteoblast-specific gene expression in non-osteoblastic cells. J Biol Chem **279,** 47109, 2004.
54. Eggermann, J., Kliche, S., Jarmy, G., Hoffmann, K., Mayr-Beyrle, U., Debatin, K.M., Waltenberger, J., and Beltinger, C. Endothelial progenitor cell culture and differentiation *in vitro*: a methodological comparison using human umbilical cord blood. Cardiovasc Res **58,** 478, 2003.
55. Hristov, M., Erl, W., and Weber, P.C. Endothelial progenitor cells: mobilization, differentiation, and homing. Arterioscler Thromb Vasc Biol **23,** 1185, 2003.
56. Nguyen, V.A., Furhapter, C., Obexer, P., Stossel, H., Romani, N., and Sepp, N. Endothelial cells from cord blood CD133+CD34+ progenitors share phenotypic, functional and gene expression profile similarities with lymphatics. J Cell Mol Med **13,** 522, 2009.

Address correspondence to:
Stephen M. Warren, MD
Institute of Reconstructive Plastic Surgery Laboratories
New York University Langone Medical Center
560 First Ave, TH-169
New York, NY 10016

E-mail: stephen.warren.md@gmail.com

Received: May 24, 2012
Accepted: January 16, 2013
Online Publication Date: March 18, 2013